The Abdus Salam
International Centre for Theoretical Physics

United Nations
Educational, Scientific
and Cultural Organization

International Atomic
Energy Agency

SMR.1676 - 21

8th Workshop on Non-Linear Dynamics and Earthquake Prediction

3 - 15 October, 2005

Memory, reciprocity and double Green function in diffusion, elastic and electromagnetic fields

Experimental and Theoretical memory diffusion of water in sand

Michele Caputo
Universita degli Studi di Roma "La Sapienza"
Dipartimento di Fisica
Piazzale Aldo Moro 2
00185 Roma
Italy

Eighth Workshop on Non Linear Dynamics and Earthquake Prediction , ICTP, Trieste, 03-15 October 2005

Memory, reciprocity and double Green function in diffusion, elastic and electromagnetic fields.

Michele Caputo
Department of Physics, University of Rome La Sapienza, Piazzale A. Moro 2, 00185, Roma, Italy (correspondence address); and Department of Geology and Geophysics, Texas A&M University, College Station, 77843, Texas.
mcaputo@g24ux.phys.uniroma1.it el.390649913516

$$a(t)*q(x,t) = - b(t)*grad\, p(x,t) \qquad (1)$$

$$div\, q + \partial m / \partial t = 0 \qquad (2)$$

$$(m{=}m_t{-}m_0) \;\; ap = \alpha m, \;\; ap(x,0) = \alpha m(x,0) = 0 \qquad (3)$$

Taking the Laplace Transform (LT) of equation1 (1) through (3)

we obtain

$$sG(s)P = P_{xx} \qquad (4)$$

$$G(s) = A(s)/B(s) \qquad (5)$$

$$A(s) = \mathrm{LT}\; a(t), \qquad B(s) = \mathrm{LT}\; b(t)$$

The solution of equation (4) is

$$P = C_1 \exp(\sqrt{Gs}x) + C_2 \exp(-\sqrt{Gs}x) \qquad (6)$$

where C_1 and C_2 are functions of s.

Assuming further $P(0,s) = B_0(s)$, $P(h,s) = B_h(s)$

$$P(0,s)=C_1+C_2 =B_0(s)$$

$$P(h,s)=C_1exp((Gs)^{1/2}h)+C_2\, exp(-(Gs)^{1/2}h)+K/s =B_h(s) \qquad (7)$$

which give

$$C_1=[B_h-B_0\, exp(-Gs)^{1/2}h)]/[exp\, ((Gs)^{1/2}h) -exp(-(Gs))^{1/2}h] \quad (8)$$

$$C_2=B_0 -[B_h-B_0\, exp(-Gs)^{1/2}h)]/[exp\, ((Gs)^{1/2}h) -exp(-(Gs))^{1/2}h]$$

$$sG(x,s)P_1 = P_{1xx} \qquad (9)$$

$$sG(x,s)P_2 = P_{2xx}$$

$$P_1P_{2xx} - P_{1xx}P_2 = 0$$

where the factor $sG(x,s)$, that is the mathematical expression of

$$P_1P_{2xx} - P_{1xx}P_2 = d(P_1P_{2x} - P_{1x}P_2)/dx = 0$$

or integrating on x from zero to h

$$\int_0^h (P_1P_{2xx} - P_{1xx}P_2)dx = [\ (P_1P_{2x} - P_{1x}P_2)\ ]_{x=h} - [\ (P_1P_{2x} - P_{1x}P_2)\ ]_{x=0} = 0$$
(10)

$$(P_{1h}P_{2xh} - P_{1xh}P_{2h}) - (P_{10}P_{2x0} - P_{1x0}P_{20}) = 0$$

$$P_{1h}P_{2xh} - P_{1xh}P_{2h} = 0 \qquad (11)$$

or

$$P_{2xh} = P_{1xh} P_{2h} / P_{1h} \tag{12}$$

$$c_{1h} P_{2xh} / s - P_{1xh} P_{2h} + P_{1x0} P_{20} = 0 \tag{13}$$

$$P_{2xh} = s[P_{1xh} P_{2h} - P_{1x0} P_{2o}] / c_{1h} \tag{14}$$

$$c_{3h} P_{2xh} - P_{3xh} P_{2h} - c_{30} P_{2x0} / s + P_{3x0} P_{20} = 0 \tag{15}$$

$$c_{1h} P_{2xh} / s - P_{1xh} P_{2h} + P_{1x0} P_{20} = 0$$

$$c_{3h} P_{2xh} - P_{3xh} P_{2h} - c_{30} P_{2x0} / s + P_{3x0} P_{20} = 0$$

$$c_{3h} [s P_{1xh} P_{2h} - s P_{1x0} P_{20}] / c_{1h} - P_{3xh} P_{2h} - c_{30} P_{2x0} / s + P_{3x0} P_{20} = 0$$

$$P_{2x0} = \{\ [c_{3h} s P_{1xh} / c_{1h} - P_{3xh}] P_{2h} - [c_{3h} s P_{1x0} / c_{1h} - P_{3x0}] P_{20}\ \} / (c_{30} / s)$$

(16)

$$P_{2x0} = s\{\ [s P_{1xh} - P_{3xh}] P_{2h} - [s P_{1x0} - P_{3x0}] P_{20}\ \} / c_{30} \tag{17}$$

$$Q_{20} = -P_{2x0} a / \alpha G(s)) \tag{18}$$

$$a(t) = \gamma \delta(t) + H(t) \varepsilon\ t^{-n_1} / \Gamma(1-n_1) + H(t) g \int_{\lambda}^{\mu} t^{-u} du / \Gamma(1-u)$$

$$b(t) = c\delta(t) + H(t) d\,\partial t^{-n_2} / \Gamma(1-n_2) + H(t) h \int_{\varphi}^{\psi} t^{-v} dv / \Gamma(1-v)$$

(19)

$n_1 \in [0.1[$, $n_2 \in [0,1[$, $\varphi \in [0,1[$, $\psi \in [0,1[$,

$\lambda \in [0,1[$, $\mu \in [0,1[$

$$[\gamma + \varepsilon\,\partial^{n_1}/\partial t^{n_1} + g\int_{\lambda}^{\mu} \partial^{u}/\partial t^{u} du]q = -[c + d\,\partial^{n_2}/\partial t^{n_2} + h\int_{\varphi}^{\psi} \partial^{v}/\partial t^{v} dv]\,gra$$

(20)

$$a[(\gamma + \varepsilon s^{n_1} + g(s^{\mu} - s^{\lambda})/\log s]/\alpha[c + d\,s^{n_2} + h(s^{\psi} - s^{\varphi})/\log s] = G(x,s)$$

(21)

$$g = h = 0 \qquad (22)$$

$$1/G(x,s) = \alpha[c + d\,s^{n_2}]/a[(\gamma + \varepsilon s^{n_1}] \qquad (23)$$

LT $^{-1}$ $(1//G(s) = (\alpha c/a\varepsilon)[\delta(t) + (c/d - \gamma/\varepsilon)(\varepsilon/\gamma)$ [t-

$$+ (\sin\pi v/\pi v)\int_{0}^{\infty} (1 - \exp(-((\gamma/\varepsilon)u)^{1/v} t))du/(\gamma/\varepsilon)u^{1/v}(u^2 + 2u\cos\pi v + 1)$$

]] (24)

Appendix

$P_1(h,s) = 1/s,\ P_1(0,s) = 0;$

$C_1 = (1s)/[exp((Gs)^{1/2}h) - exp(-(Gs)^{1/2}h)],$

$C_2 = -\ (1s)/[exp((Gs)^{1/2}h) - exp(-(Gs)^{1/2}h)],$

$P_1(x,s) = (1/s)[exp((Gs)^{1/2}x) - exp(-(Gs)^{1/2}x)]$

$/[exp((Gs)^{1/2}h) - exp(-(Gs)^{1/2}h)],$

$P_{1x} = ((Gs)^{1/2}/s)\ [exp((Gs)^{1/2}x) + exp(-(Gs)^{1/2}x)]/[exp((Gs)^{1/2}h) -$

$exp(-(Gs)^{1/2}h)],$

$P_{1x0}=(2/s)\ (Gs)^{1/2}\ /[exp((Gs)^{1/2}h)\ -\ exp(-(Gs)^{1/2}h)]$, (A1)

$P_{1xh}=(1/s)(Gs)^{1/2}\ [exp((Gs)^{1/2}h)\ +\ exp(-(Gs)^{1/2}h)]/[exp((Gs)^{1/2}h)$

$-\ exp(-(Gs)^{1/2}h)]$,

and for P_3 : $P_3(h,s) = 1;\ P_3(0,s) = 1/s$

$C_1=[1-exp(-(Gs)^{1/2})/s))]/[exp((Gs)^{1/2}h)\ -\ exp(-(Gs)^{1/2}h)]$,

$C_2 = 1/s-\ [1-exp(-(Gs)^{1/2})/s]/[exp((Gs)^{1/2}h)\ -\ exp(-(Gs)^{1/2}h)]$,(A2)

$P_3(x,s) = [1-exp(-(Gs)^{1/2}))/s]/[exp((Gs)^{1/2}h)\ +$

$-\ exp(-(Gs)^{1/2}h)]exp((Gs)^{1/2}x)+$

$+[1/s\ -\ [1-exp(-(Gs)^{1/2}))/s]/[exp(Gs)^{1/2}h)\ +$

$-\ exp(-(Gs)^{1/2}h)]]\ exp(-(Gs)^{1/2}x)$

$P_{3x}\ (x,s) =\ (Gs)^{1/2}\ [1-exp(-(Gs)^{1/2})/s]\ [exp((Gs)^{1/2}x)+$

$+\ exp(-(Gs)^{1/2}x))]\ /$

$[exp((Gs)^{1/2}h)\ -\ exp((-Gs)^{1/2}h)]\ -(Gs)^{1/2}\ exp(-(Gs)^{1/2}x)/s$

$P_{3x0} = (Gs)^{1/2}[2[1\ -\ exp(-(Gs)^{1/2}h)/s]\ /[exp((Gs)^{1/2}h)\ +$

$-\ exp(-(Gs)^{1/2}h)]\ -1/s]$,

$P_{3xh} = (Gs)^{1/2}\ [exp((Gs)^{1/2}h)+exp((-Gs)^{-1/2}h)-2/s]\ /$

$[exp((Gs)^{1/2}h)\ -\ exp(-(Gs)^{1/2}h)]$

In the case the conditions (22) are enforced ($g = h = 0$, $n_1 = n_2 = v$) the LT^{-1} is reduced to that of

$$w\,[exp((w\,h) + exp(-w\,h)]/[exp(w\,h) - exp(-w\,h)], \qquad (A3)$$

$$w\,/[exp(w\,h) - exp(-w\,h)], \qquad (A4)$$

$$w\,exp(-wh)\,/[exp(w\,h) - exp(-w\,h)],\ \ w = (Gs)^{1/2} \qquad (A5)$$

Eighth Workshop on Non Linear Dynamics and Earthquake Prediction , ICTP, Trieste, 03-15 October 2005

EXPERIMENTAL AND THEORETICAL MEMORY DIFFUSION OF WATER IN SAND

G. Iaffaldano (1, 2,), M. Caputo (1) and S. Martino (3)

(1) Department of Physics, University of Rome "La Sapienza", P.le A. Moro 2, 00185 Rome, Italy.

Hydrology and Earth System Science (*in press*), 2005

(2) Department of Earth and Environmental Sciences,Section of Geophysics

Theresienstrasse 41/IV, 80333 Munich (Germany),

(3) Department of Earth Sciences, University of Rome "La Sapienza", P.le A. Moro 2,

00185 Rome, Italy.

Abstract

The basic equations used to study the fluid diffusion in porous media have been set by Fick and Darcy in the mid of the XIXth century but some data on the flow of fluids in rocks exhibit properties which may not be interpreted with the classical theory of propagation of pressure and fluids in porous media [*Bell and Nur*, 1978; *Roeloffs*, 1988].

Concerning the fluids and the flow, some fluids carry solid particles which may obstruct some of the pores diminishing their size or even closing them, some others may chemically and physically react with the medium enlarging the pores; so permeability changes during time and the flow occurs as if the medium had a memory.

The scope of this paper is to show, with experimental data, that the permeability of sand layers may decrease due to reassessment of the grains and consequent compaction as shown qualitatively by Elias and Hajash [1992], He [2001] and He et al. [2002]. We also provide a memory model for diffusion of fluids in porous media which fits well the flux rate observed in five laboratory experiments of diffusion of water in sand. Finally we show that the flux rate variations observed during the experiments are compatible with the compaction of sand, due to the amount of fluid which went through the grains locally, and therefore with the reduction of porosity. All the experiments have been set in the Applied Geology Laboratory at the department of Earth Sciences of the University "La Sapienza" of Rome".

1. Introduction

The basic equations used to study the fluid diffusion in porous media have been set by Fick and Darcy in the mid of the XIXth century. Many authors contributed in various forms, using Darcy's law which states that the flux is proportional to the pressure gradient, to set equations rigorously representing the interaction between the porous media and the flow of fluid through it and obtained equations solutions in many interesting cases [*Bear*, 1972; *Sposito*, 1980; *Steefel and Lasaga*, 1994; *Dewers and Ortoleva*, 1994; *Indelman and Abramovici*, 1994; *Mainardi et al.*, 1998; *Cushman and Moroni*, 2001; *Moroni and Cushman* 2001]. In spite of this, some data on the flow of fluids in rocks exhibit properties which may not be interpreted with the classical theory of propagation of pressure and fluids in porous media [*Bell and Nur*, 1978; *Roeloffs*, 1988] nor adequately with many of the new theories.

Concerning the fluids and the flow, some fluids carry solid particles which may obstruct some of the pores diminishing their size or even closing them, some others may chemically and physically react with the medium enlarging the pores; so permeability changes during time and the flow occurs as if the medium had a memory, intending that at any instant the process of diffusion is also affected by the previous local value of pressure and flow of the fluid. This phenomenon would be taken into account when writing equations for diffusion of fluids in porous media.

The scope of this paper is to show quantitatively, with experimental data, that the permeability of sand layers may decrease due to reassessment of the grains and consequent mechanical compaction [*Elias and Hajash*, 1992, *He* 2001, *He et al.* 2002].]. We will provide, by rewriting the constitutive equation of diffusion with memory formalism, a new model for diffusion of fluids in porous media [*Caputo*, 2000] in order to describe permeability changes observed in the flux rate through the sand samples.

2. The laboratory experiments

The experiments were designed to obtain flow measures through a porous layer with constant hydraulic pressure difference between the boundary surfaces of the samples.

In order to obtain considerable flux the porous medium selected is sand which showed an adequate compaction and therefore considerable permeability and flux rate variations during the experiments. The grain size distributions shown in Figure 1.a and 1.b were measured by sieves; the percentiles of the cells are shown on top of histogram.

Sand density was estimated to be $\rho_S = (2.4 \pm 0.1) gr / cm^3$.

We used water as fluid, its temperature during all experiments was $(19 \pm 1)\,°C$.

A schematic description of the instrument assembled for the diffusion experiments is shown in Figure 2.

Figure 2 : experimental device

Water-saturated sand is kept in the *cell for medium*, a cylinder shaped metal box of height $l = (11.6 \pm 0.1)\ cm$ and surface's inner diameter $D_I = (10.1 \pm 0.1)\ cm$; R, R_I and R_U are water-taps and R is also water source; T is a tank with input gate I and output gate U; $H = (212 \pm 1)\,cm$. To obtain constant hydraulic pressure on the boundary surface in $x = l$, initially, the water-taps R and R_U are turned on while R_I is off so that the column between T and R_I gradually is filled with water.

The water flow through R is sufficiently large that takes few seconds for the column to be filled, after this time the surplus flows out from the gate U.

Opening R_I the pressure on the boundary plane in $x = l$ is equal to the pressure of a water column of height H and so water begins to flow through porous medium and runs out from R_U. Note that the column is always of height H because the surplus water flows out from the gate U. In this way a constant pressure difference is maintained between the boundary planes in $x = l$ and $x = 0$, which was verified during experiments using the pressure gauge B.

In this configuration, measures of water flow at the boundary surface in $x = 0$ were obtained by storing the water that flow through the surface in a small container with capacity of about 100 cm^3 and taking note of the relative time interval with $10^{-2}\ s$ precision chronometer.

The water mass in the filled container was measured using $10^{-4}\ g$ precision scale and flow rate measured.

In order to diminish the error of the experimenter and of the devices the water mass in each filled container was measured three times with the scale, experimenter error in starting and stopping chronometer was evaluated to be $10^{-1}\ s$ and each flow measure is the average value of three containers filled in rapid succession. The estimated relative error in the flux is then about 2%.

The following figures 3, 4, 5, 6 and 7 show all experimental data collected. In each experiment the flow measures are separated by 20 minutes, only the first measures are separated by 10 minutes. The data collection is limited to about 10 hours when the flow seems to have reached a very slow and steady rate to imply that a steady state is reached.

The solid line in each figure is the theoretical flux obtained by fitting to the experimental data the memory model which will be introduced I the following.

Note that for each experiment in the first few hours the flux rate steadily decreases defining a transient phase. It appears that in several hours, seemingly less than 10, after the transient phase, the flux establishes to a value that is about 70% of the initial one, only in experiment 5 it is about 46% of initial value. Opening the *cell for medium* after each experiment we observed a height reduction of the sand of about $3-4\ mm$, that is about 3% of the porous media volume, and this is an evidence of mechanical compaction.

In order to quantitatively discuss the variation of the flux rate in terms of the porous media volume reductions we used empirical Fair and Hatch law (1933) for permeability k [*Bear*, 1972]

$$k = C_M z^3/(1-z)^2 \tag{1}$$

where z is medium porosity and C_M is a geometrical medium dependent coefficient introduced to take into account the grain size distribution, grains shape and chemical properties of the medium.

The sand mass contained in the *cell for medium* in each experiment was $m = (1550 \pm 30)g$ (dry sand) and since no sand may go out from the cell during the experiment we can compute the initial (I) and final (F) saturated medium porosity:

$$z_I = \frac{V_{VI}}{V_I} = \frac{V_I - \dfrac{m}{\rho_S}}{V_I} = 1 - \frac{m}{V_I \rho_S} \tag{2}$$

$$z_F = \frac{V_{VF}}{V_F} = \frac{V_F - \dfrac{m}{\rho_S}}{V_F} = 1 - \frac{m}{V_F \rho_S} \tag{3}$$

$V_{V\_}$ is the volume of intergranular spaces of the sand. Using Fair and Hatch permeability law we estimate that the difference between initial and final values of k is

$$\Delta k_{\%} = 100 \cdot \left| \frac{k_I - k_F}{k_I} \right| = 100 \cdot \left| 1 - \frac{k_F}{k_I} \right| = 100 \cdot \left| 1 - \frac{z_F^3 (1 - z_I)^2}{z_I^3 (1 - z_F)^2} \right| \tag{4}$$

Remembering $\rho_S = (2.4 \pm 0.1) g/cm^3$, from (2) and (3) results $\Delta k_{\%} = (26 \pm 3)\%$. This permeability reduction justifies experimentally observed flux rate reduction.

3. The modeling of the flux variation

In order to model the permeability variation with a memory mechanism, meaning that at any instant the process of diffusion is affected by the previous amount of fluid which went through the pores we modified as follows the original Fick law, stating proportionality between flux and pressure gradient

$$\overline{q}(\overline{x}, t) = -c \overline{\nabla} p(\overline{x}, t) \tag{5}$$

where p is fluid pressure in the porous medium and q is fluid flow through medium, introducing in it a derivative of fractional order n [*Caputo*, 2000]:

$$\gamma \overline{q}(\overline{x}, t) = -\left[c + d \frac{\partial^n}{\partial t^n} \right] \overline{\nabla} p(\overline{x}, t) \tag{6}$$

$$a p(\overline{x}, t) = \alpha \rho(\overline{x}, t) \tag{7}$$

$$div \overline{q}(\overline{x}, t) + \frac{\partial \rho(\overline{x}, t)}{\partial t} = 0 \tag{8}$$

where ρ is variation of fluid density in medium from the undisturbed condition while γ, c and d are real numbers modulating memory formalism, α/a is the bulk modulus of the fluid.

The fractional oreder derivative is defined as follows [*Caputo,* 1967; *Caputo*, 1969; *Podlubny*, 1999]

$$f^{(n)}(t) = \frac{\partial^n f(t)}{\partial t^n} = \frac{1}{\Gamma(1-n)} \int_0^t \frac{\dot{f}(u)}{(t-u)^n} du \tag{9}$$

where $n \in [0,1[$ and Γ is the Gamma function. In practice the derivative of fractional order $f^{(n)}(t)$ is constructed with a weighted mean of the first order derivative $\dot{f}(u)$ in the time interval $[0,t]$, which is a sort of feedback system. That is, the values of $\dot{f}(u)$ at time u far apart from t are given smaller weight than those at time u closer to t. Hence, the weights are increasingly smaller with increasing time separation from t to imply that the effect of past is fading with increasing time. When $n = 0$ and $f(0) = 0$ the fractional derivative reduce to the functions themselves.

Importantly, the weights multiplying the first order derivative $\dot{f}(u)$ inside the integral appearing in equation (6) can be chosen in many ways. The definition adopted in equation (6) has been set by Caputo (1967) and is appropriate because it is algebraically simple, allows easy solutions and has commonly been applied in previous scientific studies dealing with electromagnetism [*Jacquelin*, 1984], biology [*Caputo*, 2002b; *Cesarone*, 2002] and economy [*Caputo and Kolari*, 2001; *Caputo*, 2002a; *Caputo and Di Giorgio*, 2003].

It is noteworthy to observe how the memory functions capture the past. What the fractional derivative memory functions are remembering is their past values as defined by equation (6), which implies that the function is constructed by adding to the initial value the successive weighted increments over time. The increments per unit time are represented by the first order derivative under the integral sign and the weights are represented by the factor of the first order derivative in equation (9), which are decreasing with increasing time separation from t. Thus, a variable's value is a weighted mean of its past value.

In order to fit experimental data with memory model we find in the *Appendix A* the Green function of the flux $q(0,t)$ when diffusion occurs through a slab of thickness l with pressure boundary conditions

$$p(0,t) = 0 \tag{10}$$

$$p(l,t) = K = \text{constant} \tag{11}$$

and initial pressure condition

$$p(x,0) = K = \text{constant} \tag{12}$$

Figure 8: porous slab

In order to obtain the flux $q(0,t)$ we solve the equations (6) – (8) in the Laplace Transform (LT) domain obtaining

$$P(x,s)=\frac{K}{s}\left[\frac{e^{Bs^{\nu}(x-l)}-e^{Bs^{\nu}(l-x)}}{e^{Bs^{\nu}l}-e^{-Bs^{\nu}l}}+1\right] \tag{13}$$

and

$$Q(0,s)=-\frac{dKB}{\gamma s^{\nu}}\left[\frac{1+e^{2Bs^{\nu}l}}{e^{2Bs^{\nu}l}-1}\right] \tag{14}$$

where

$$B=\left[\frac{\gamma a}{\alpha d}\right]^{\frac{1}{2}},\ \nu=\frac{1-n}{2} \tag{15}$$

and s is the LT variable.

The LT^{-1} of (15) is found in the *Appendix B* and the following expression of boundary flux is obtained

$$q(0,t)=-\frac{dBK}{2\pi\gamma}\int_{0}^{+\infty}\frac{e^{-rt}}{r^{\nu}}\cdot\frac{2sin(\pi\nu)\left[e^{2Mr^{\nu}}-1\right]+4sin\left(Nr^{\nu}\right)\cos(\pi\nu)e^{Mr^{\nu}}}{e^{2Mr^{\nu}}+1-2\cos\left(Nr^{\nu}\right)e^{Mr^{\nu}}}dr \tag{16}$$

with

$r=$ modulus of s

$M=2Bl\cos(\pi\nu)$

$N=2Bl\sin(\pi\nu)$

Note that in equation (9) $a/\alpha=\rho_F z/k_E$, where ρ_F is fluid density and k_B is bulk modulus of fluid; water values are $\rho_F=1\left(g\cdot cm^{-3}\right)$ and $k_B=2.08\cdot 10^{10}\left(g\cdot cm^{-1}\cdot s^{-2}\right)$ [*Domenico and Schwartz*, 1997]. Therefore $B=(\gamma/d)(\rho_F z/k_E)^{\frac{1}{2}}$ and, assuming for sand $z=0.35$ [*Bear*, 1972], the boundary flux theoretical solution $q(0,t)$ depends on memory parameter d/γ and the order of fractional derivative n through $\nu=(1-n)/2$.

With extreme values theorem it is seen that

$$\lim_{s\to 0}sQ(0,s)=\lim_{t\to+\infty}q(0,t)=0 \tag{17}$$

$$\lim_{s\to\infty}sQ(0,s)=\lim_{t\to 0}q(0,t)=-\infty \tag{18}$$

4. Fitting the model to the experimental data

The experimental data show that in several hours flux seems close to stabilization and, since we will describe only the transient phase of diffusion ($c = 0$), we obtained the data, to fit to the model, by subtracting the original data the average of the last few hours of flux (let's call it q_{AS}). The data of the five experiments run indicate that q_{AS} is a good candidate for asymptotic flux and new data are good to represent the diffusion transient phase we want to describe.

In order to best fit memory model to experimental data we minimized the following two variables function

$$AD\left(\nu, \frac{d}{\gamma}\right) = \frac{1}{N_D}\sum_{i=1}^{N_D}\left|ED_i - q\left(t_i, \nu, \frac{d}{\gamma}\right) - q_{AS}\right| \tag{19}$$

where N_D is the number of experimental data for each experiment, ED_i are the data obtained in the laboratory at the time t_i.

The results of fitting for the five experiments are shown in the following table

	n	$\frac{d}{\gamma}\left(s^{1+n}\right)$	$AD\left(g \cdot s^{-1}\right)$	$q_{AS}\left(g \cdot s^{-1}\right)$
Experiment 1	0.46 ± 0.01	0.008 ± 0.001	0.8	30.3
Experiment 2	0.58 ± 0.01	0.014 ± 0.002	0.41	27.1
Experiment 3	0.54 ± 0.01	0.012 ± 0.002	0.52	27.5
Experiment 4	0.54 ± 0.01	0.010 ± 0.001	0.55	27.2
Experiment 5	0.58 ± 0.02	0.046 ± 0.003	0.8	27.1

Note that experiment 5 is a bit different from the others, in fact the initial flux is higher and the transient reaches steady state at about 46% of the initial value while the others reach steady state at about 71% the initial value. Taking into account only the first four experiments it results that both for n and d/γ the average quadratic discrepancy (AQD) is compatible with the relative average value (AV); values are shown in the table below

	n	$\frac{d}{\gamma}\left(s^{1+n}\right)$
Average value	0.53	0.011
AQD	0.04	0.002

The procedure to obtain best fits is indicated in the *Appendix C*.

5. Conclusions

In all experiments we have observed that flux decreases in time to about 71% of initial value and that the volume of sand reduces of about 3%; moreover, using empirical Fair and Hatch law for permeability, the sand volume and flux reductions seem compatible; which proves that mechanical compaction occurring during diffusion is cause by the permeability changes which in turn cause the flux variations.

The classic theory, in the case of constant diffusivity, with constant boundary and initial conditions, would give a constant flux contrary to the results of our laboratory experiments. One would have to introduce in the equations a time variable diffusivity which is a priory unknown and would have to be determined monitoring the permeability changes caused by the flux in the sand.

Note that for each experiment the value of the minimum *AD* numerically computed is about 2% of average observed flux and that the order of the fractional derivatives has a standard deviation of 0,048 or 9% of the average value which, taking into account the variety of samples, is rather satisfactory and, with the low value of *AD*, confirms the validity of the model.

We have also seen that, with the boundary and initial conditions used, the relaxation time of the flux, that is the time to reach stability, is about 10 hours which in turn implies that the compaction of the sand in the sample has the same relaxation time. However in terms of the memory model the flux and the associated relaxation time are now defined by two parameters, and not only one as in the classic theory; the parameters are the order of fractional derivative n and $d\mu/\gamma\rho_F$, where μ is the viscosity of the fluid, which are called pseudodiffusivity [*Caputo*, 2000].

Appendix A

It is useful to rewrite memory relations in one dimension:

$$\gamma q(x,t) = -\left[c + d\frac{\partial^n}{\partial t^n}\right]\frac{\partial p(x,t)}{\partial x} \tag{A.1}$$

$$ap(x,t) = \alpha\rho(x,t) \tag{A.2}$$

$$\frac{\partial q(x,t)}{\partial x} + \frac{\partial \rho(x,t)}{\partial t} = 0 \tag{A.3}$$

In this appendix we find the LT of the Green function of the flux resulting from (A.1) – (A.3) with boundary and initial condition given by (11) – (13).

The LT of (A.1), (A.2) and (A.3) are respectively

$$\gamma Q(x,s) = -(c + ds^n)P_x(x,s) \tag{A.4}$$

$$aP(x,s) = \alpha R(x,s) \tag{A.5}$$

$$Q_x(x,s) + sR(x,s) - \rho(x,0) = 0 \tag{A.6}$$

With $R(x,s) = LT[\rho(x,s)]$.

Substituting (A.6) in (A.5) we find

$$aP = -\frac{\alpha}{s}[Q_x(x,s) - \rho(x,0)] \tag{A.7}$$

Differentiating (A.4) with respect to x and substituting in (A.7) we obtain

$$\frac{(c + ds^{n_2})}{\gamma}P_{xx} = \frac{1}{\alpha}[asP - \alpha\rho(x,0)] \tag{A.8}$$

Here, in order to reduce the number of free parameters and to simplify the formulae, we set $c = 0$ which is justified as follow: it seems that in several hours, seemingly less than 10 hours, the flux stabilizes but we cannot rule out that it is asymptotically nil. If the flux were constant after 10 hours then the rigorous solution requires that $c \neq 0$, which implies that asymptotically the flux is constant as required by Darcy's law which does not apply here. We have two options:

1. consider the transient phase which is asymptotically nil
2. consider that after the transient phase the flux stabilizes

However, since we have no indication of the asymptotic value, also for simplicity of computation, we studied only the transient phase and set $c = 0$.

So equation (A.8) becomes

$$\frac{d}{\gamma} s^{n_2} P_{xx} = \frac{a}{\alpha} sP - \rho(x,0) \tag{A.9}$$

substituting (A.2) into (A.9) and renaming $n_2 = n$ we find

$$P_{xx} = \frac{\gamma a}{\alpha d}\left[s^{1-n}P - s^{-n} p(x,0)\right] \tag{A.10}$$

The general solution of (A.10) is

$$P(x,s) = C_1(s)e^{Bs^{\nu}x} + C_2(s)e^{-Bs^{\nu}x} + \frac{K}{s} \tag{A.11}$$

where $B = [\gamma a/\alpha d]^{1/2}$ and $\nu = (1-n)/2$.

Substituting the boundary conditions (11) and (12) in equation (A.11) we obtain

$$C_1(S) = -\frac{K}{s}\frac{e^{-Bs^{\nu}l}}{e^{-Bs^{\nu}l} - e^{Bs^{\nu}l}} \tag{A.12}$$

$$C_2(S) = \frac{K}{s}\frac{e^{Bs^{\nu}l}}{e^{-Bs^{\nu}l} - e^{Bs^{\nu}l}} \tag{A.13}$$

and so general solution (A.11) becomes

$$P(x,s) = \frac{K}{s}\left[\frac{e^{Bs^{\nu}(x-l)} - e^{Bs^{\nu}(l-x)}}{e^{Bs^{\nu}l} - e^{-Bs^{\nu}l}} + 1\right] \tag{A.14}$$

Differentiating (A.14) with respect to x and substituting in (A.4) we obtain

$$Q(x,s) = -\frac{dKB}{\gamma s^{\nu}}\left[\frac{e^{Bs^{\nu}(x-l)} + e^{Bs^{\nu}(l-x)}}{e^{Bs^{\nu}l} - e^{-Bs^{\nu}l}}\right] \tag{A.15}$$

Appendix B

In this appendix we find the LT^{-1} of (15), to be fit to experimental data, by integrating $e^{st}Q(0,s)$ along the path of figure B.1 below.

When the radius R_1 of the inner circle Γ_1 goes to infinity and the radius R_2 of the outer circle Γ_2 goes to zero the residual theorem (RT) states that the integral is equal to the sum of residuals inside the path.

Path of integration in figure B.1 can be divided as follow

$$\Gamma_T = \Gamma_1 + \Gamma_{FH} + \Gamma_{HA} + \Gamma_{AB} + \Gamma_{BD} + \Gamma_{DE} \tag{B.1}$$

and when $R_1 \to 0$ we find that $\Gamma_{BD} \to \Gamma_{CD}$ and $\Gamma_{HA} \to \Gamma_{HK}$. Let's compute the contributes of integration along Γ_1, Γ_{CD} and Γ_{HK}.

Figure B.1: path of integration in the complex plane

Concerning the integral along Γ_1, when the radius R_1 goes to zero the Taylor series of $Q(0,s)$ near $s = 0$ is

$$Q(0,s) \cong -\frac{2dKB}{\gamma s^{\nu}}\left[\frac{1}{2Bls^{\nu} + o\left(s^{2\nu}\right)}\right] \tag{B.2}$$

Because of $\nu \in \left]0,\frac{1}{2}\right[$, we obtain

$$\lim_{s\to 0} sQ(0,s) = \lim_{R_1\to 0} -\frac{2dKB}{\gamma}\frac{s^{1-\nu}}{\left(2Bls^{\nu} + o\left(s^{2\nu}\right)\right)} = 0 \tag{B.3}$$

and so integral along Γ_1 is nil.

To compute integrals along Γ_{CD} and Γ_{HK}, it is useful to rewrite $e^{st}Q(0,s)$ with $s = R_2 e^{i\vartheta}$:

$$-\frac{dBK}{\gamma} iR_2 e^{i\vartheta} e^{R_2 t\cos(\vartheta)} e^{iR_2 t\sin(\vartheta)} \frac{1 + e^{2lBR_2^{\nu}\cos(\vartheta\nu)} e^{i2lBR_2^{\nu}\sin(\vartheta\nu)}}{R_2^{\nu} e^{i\vartheta\nu}\left(e^{2lBR_2^{\nu}\cos(\vartheta\nu)} e^{i2lBR_2^{\nu}\sin(\vartheta\nu)} - 1\right)} \tag{B.4}$$

when R_2 goes to infinity imaginary exponential can be neglected because limited in $[-1;1]$, $\cos(\vartheta\nu) \in \left]0,1\right[$ because $\vartheta \in \left]\frac{\pi}{2},\pi\right[\cup \left]-\pi,-\frac{\pi}{2}\right[$ and $\nu = \frac{1-n}{2} \in \left]0,\frac{1}{2}\right[$. So we obtain

$$\lim_{R_2\to+\infty} -\frac{dBK}{\gamma} iR_2 e^{i\vartheta} e^{R_2 t\cos(\vartheta)} e^{iR_2 t sin(\vartheta)} \frac{1+e^{2lBR_2^\nu \cos(\vartheta\nu)} e^{i2lBR_2^\nu sin(\vartheta\nu)}}{R_2^\nu e^{i\vartheta\nu}\left(e^{2lBR_2^\nu \cos(\vartheta\nu)} e^{i2lBR_2^\nu sin(\vartheta\nu)}-1\right)} = 0 \quad \text{(B.5)}$$

and integrals along Γ_{CD} and Γ_{HK} are nil because function inside integral sign is nil.

Function $e^{st}Q(0,s)$ has no singularity in the complex plain except in the origin, already analyzed. For RT, renaming $e^{st}Q(0,s)=I(s)$, we have

$$\lim_{\substack{R_1\to0\\R_2\to+\infty}} \left[\int_{\Gamma_T} I(s)ds\right] = \lim_{\substack{R_1\to0\\R_2\to+\infty}} \left[\int_{-iR_2}^{+iR_2} I(s)ds + \int_{\Gamma_{DE}} I(s)ds + \int_{\Gamma_{FH}} I(s)ds\right] = 0 \quad \text{(B.6)}$$

and so, dividing all for 2π

$$TL^{-1}[Q(0,s)] = \lim_{\substack{R_1\to0\\R_2\to+\infty}} \frac{1}{2\pi i}\left[-\int_{\Gamma_{DE}} I(s)ds - \int_{\Gamma_{FH}} I(s)ds\right] \quad \text{(B.7)}$$

For the integral along Γ_{DE} we set $s=re^{i\pi}$ and obtain

$$I\left(re^{i\pi}\right) = I_{DE}(r) = -\frac{dBK}{\gamma}\frac{e^{-rt}}{e^{i\pi\nu}r^\nu}\frac{\left(1+e^{Zr^\nu}\right)}{\left(e^{Zr^\nu}-1\right)} \quad \text{(B.8)}$$

with

$Z = M + iN$

$M = 2Bl\cos(\pi\nu)$

$N = 2Bl\sin(\pi\nu)$

For the integral along Γ_{FH} we set $s=re^{-i\pi}$ and in the same way we have

$$I\left(re^{-i\pi}\right) = I_{FH}(r) = -\frac{dBK}{\gamma}\frac{e^{-rt}}{e^{-i\pi\nu}r^\nu}\frac{\left(1+e^{Z^*r^\nu}\right)}{\left(e^{Z^*r^\nu}-1\right)} \quad \text{(B.9)}$$

Substituting (B.8) and (B.9) in (B.7) we obtain

$$TL^{-1}[Q(0,s)] = q_1(0,t) = \frac{1}{2\pi i}\int_0^{+\infty}\left[I_{FH}(r) - I_{DE}(r)\right]dr \quad \text{(B.10)}$$

Renaming $\omega = \pi\nu$ we have

$$I_{FH}(r) - I_{DE}(r) = \left[-\frac{dBK}{\gamma} \frac{e^{-rt}}{r^{\nu}} \right] \cdot \left[\frac{e^{i\omega}\left(1 + e^{Z^* r^{\nu}}\right)}{e^{Z^* r^{\nu}} - 1} - \frac{e^{-i\omega}\left(1 + e^{Z r^{\nu}}\right)}{e^{Z r^{\nu}} - 1} \right] =$$

$$= Y(r) \cdot \left[\frac{e^{i\omega}\left(1 + e^{Z^* r^{\nu}}\right) \cdot \left(e^{Z r^{\nu}} - 1\right) - e^{-i\omega}\left(1 + e^{Z r^{\nu}}\right) \cdot \left(e^{Z^* r^{\nu}} - 1\right)}{\left(e^{Z^* r^{\nu}} - 1\right) \cdot \left(e^{Z r^{\nu}} - 1\right)} \right] \qquad \text{(B.11)}$$

with

$$Y(r) = \left[-\frac{dBK}{\gamma} \frac{e^{-rt}}{r^{\nu}} \right]$$

Renaming $i \cdot NUM(r)$ the upper part of the ratio in (B.11) and $DEN(r)$ the lower part in the same ratio we obtain

$$i \cdot NUM(r) = e^{i\omega}\left(e^{Z r^{\nu}} - 1 + e^{2Mr^{\nu}} - e^{Z^* r^{\nu}}\right) - e^{-i\omega}\left(e^{Z^* r^{\nu}} - 1 + e^{2Mr^{\nu}} - e^{Z r^{\nu}}\right) =$$

$$= e^{i\omega}\left(e^{2Mr^{\nu}} - 1 + 2i sin\left(Nr^{\nu}\right) e^{Mr^{\nu}}\right) - e^{-i\omega}\left(e^{2Mr^{\nu}} - 1 - 2i \sin\left(Nr^{\nu}\right) e^{Mr^{\nu}}\right) =$$

$$= i \cdot \left[2\sin(\omega)\left(e^{2Mr^{\nu}} - 1\right) + 4\cos(\omega)\sin\left(Nr^{\nu}\right) e^{Mr^{\nu}}\right. \qquad \text{(B.12)}$$

and

$$DEN(r) = \left(e^{Z^* r^{\nu}} - 1\right) \cdot \left(e^{Z r^{\nu}} - 1\right) = e^{2Mr^{\nu}} - 2\cos\left(Nr^{\nu}\right) \cdot e^{Mr^{\nu}} + 1 \qquad \text{(B.13)}$$

So finally we have

$N = 2B\ell \sin \pi\nu$
$M = 2B\ell \cos \pi\nu$

$$q(0,t) = -\frac{dBK}{2\pi\gamma} \int_0^{+\infty} \frac{e^{-rt}}{r^{\nu}} \cdot \frac{2sin(\pi\nu)\left[e^{2Mr^{\nu}} - 1\right] + 4sin\left(Nr^{\nu}\right)\cos(\pi\nu) e^{Mr^{\nu}}}{e^{2Mr^{\nu}} + 1 - 2\cos\left(Nr^{\nu}\right) e^{Mr^{\nu}}} dr \qquad \text{(B.14)}$$

Appendix C

We will illustrate here how we found the minimum of AD defined in equation (19). Note that $q(0,t)$ is an integral depending on the two variables ν and d/γ and, since it is difficult and time consuming to analytically compute it, we decided to find numerically the minimum running the following routine [*Caputo and Plastino*, 1998] with MATLAB code:

1. find with several attempts a portion of domain of AD, $[\nu_1;\nu_2] \times \left[\frac{d}{\gamma_1};\frac{d}{\gamma_2}\right]$, in which the minimum is
2. chose the steps $\Delta\nu$ and $\Delta d/\gamma$ so that the portion of domain chosen becomes a bidimensional lattice as shown in figure 9

Figure C.1: bidimensional lattice

3. Start research computing AD in a point (gray rectangle in figure C.2) and in the eight neighborhoods of the lattice (black circles)
4. Select among these the point with the minimum AD (rectangle in figure C.3)
5. Compute AD in neighborhoods of previous step selected point (black circles in figure C.3), excluding those already computed (gray circles in figure C.3)
6. Repeat steps 4 and 5 until a point is selected twice consecutively; this is the point of minimum in the lattice.

Figure C.2: starting point and its neighborhoods

Figure C.3: selected point and its neighborhoods

Note that there can be in the lattice other points of local minimum for AD different from the absolute one, these points are traps and stop routine giving wrong results. In order to make sure that the point found at the end of the run was the absolute minimum we started from different points of the same lattice and made sure that the final point was the same in any case.

Glossary

ρ_S	$\left[g \cdot cm^{-3}\right]$	Mass of sand per unit volume
k	$\left[cm^2\right]$	Permeability
z	[dimensionless]	Porosity
$q(x,t)$	$\left[g \cdot s^{-1} \cdot cm^{-2}\right.$	Fluid mass flow rate in porous medium
$p(x,t)$	$\left[g \cdot s^{-2} \cdot cm^{-1}\right.$	Pressure of the fluid
$\rho(x,t)$	$\left[g \cdot cm^{-3}\right]$	Variation of fluid mass per unit volume in the porous medium from the undisturbed condition
ρ_F	$\left[g \cdot cm^{-3}\right]$	Mass of fluid per unit volume
k_B	$\left[g \cdot s^{-2} \cdot cm^{-1}\right.$	Bulk modulus of fluid
μ	$\left[g \cdot s^{-1} \cdot cm^{-1}\right]$	Viscosity of fluid
$\frac{d\mu}{\gamma\rho_F}$	$\left[s^n \cdot cm^2\right]$	Pseudodiffusivity

References

Bear J.: *Dynamics of fluids in porous media*, Elsevier, 1972.

Bell M., Nur A.: *Strength changes due to reservoir induced pore pressure and stresses and application to Lake Oroville*, J. Geophys. Res., 83, 4469-4483, 1978.

Caputo M.: *Linear model of dissipation whose Q is almost frequency independent*, Geophys. J. R. Astr. Soc., 13, 529-539, 1967.

Caputo M.: *Elasticità e dissipazione*, Zanichelli, 1969.

Caputo M., Plastino W.: *Rigorous time domain responses of polarizable media*, Annali di Geofisica, 41, 3, 399-407, 1998.

Caputo M.: *Models of flux in porous media with memory*, Water Resources Research, 3, 693-705, 2000.

Caputo M., Kolari J.: *An analytical model of the Fisher equation with memory function*, Alternative Perspectives on Finance and Accounting, 1, 1-16, 2001.

Caputo M.: *Economy equilibrium equations with memory*, National Academy of Lincei, Italy, 2002a.

Caputo M.: *Evolutionary population growth with memory in a limited habitat*, National Accademy of Lincei, 2002b.

Caputo M. , Di Giorgio G.: *Monetary Policy, Memory and Output Dynamics*, in preparation, 2003.

Caputo M., Plastino W.: *Rigorous time domain responses of polarizable media*, Annali di Geofisica, 41, 3, 399-407, 1998.

Cesarone F.: *Modello di diffusione con memoria in membrane biologiche*, Degree thesis, Advisors: Proff. Caputo M. e Cametti C., University of Rome "La Sapienza", 2002.

Cushman, J.H., Moroni, M.: *Statistical mechanics with 3D-PTV experiments in the study of anomalous dispersion*: Part I, 13(1): 75-80, Theory. Phys. Fluids, 2001.

Dewers T., Ortoleva P.: *Non linear dynamical aspects of deep basin hydrology: fluid compartment formation and episodic fluid release*, Am. J. Sc., 294, 723-755, 1994.

Domenico P.A., Schwartz F.W.: *Physical and Chemical Hydrogeology*, John Wiley, New York, 1997.

Elias B.P., Hajash A.Jr: *Changes in quartz solubility and porosity due to effective stress: An experimental investigation of pressure solution*, Geology, 20, 451-454, 1992.

He W.: *Experimental and theoretical modeling of creep compaction of quartz sand: rate laws and evolution of porosity and fluid chemistry*, Degree thesis, Advisor: Prof. Hajash A. Jr, Texas A&M University, 2001.

He W., Hajash A., Sparks D.: *A model for porosity evolution during creep compaction of sandstone*, Earth and Planetary Sciences Letters, 197, 237-244, 2002.

Indelman P., Abramovici B.: *Non local properties of non uniform averaged flow in heterogeneous media*, Water Resources Research, 30(12), 3385-3393, 1994.

Jacquelin J.: *Use of fractional derivatives to express the properties of energy storage phenomena in electrical networks*, Laboratoires Alcatel de Marcoussis, 1984.

Moroni M., Cushman J.H.: *Statistical mechanics with three-dimensional particle tracking velocimetry experiments in the study of anomalous dispersion*, Physics of fluids, 13, 1, 2001.

Podlubny I.: *Fractional differential equations*, Academic press, 1999.

Roeloffs E. A.: *Fault stability changes induced beneath a reservoir with cyclic variations in water level*, J. Geophys. Res., 93, 2107-2124, 1998.

SpositoG.: *General criteria for the validity of the Buckingham-Darcy flow law.* Soil Sci. Soc. Am. J., 44, 1159-1168, 1980.

Steefel C.I., Lasaga A.C.: *A coupled model for transport of multiple chemical species and kinetic precipitation/ dissolution reactions with application to reactive flow in single phase hydrothermal system*, Am. J. Sc., 294, 529-592,1994.

Esperimento 4 Sabbia di Stintino gialla (S.S.G.4)

$h = 210.20 \pm 0.05$ (cm)

$n = 0.4300 \pm 0.0025$

$B = 0.00040 \pm 0.00005$ (s)

$D = 0.00185 \pm 0.00005$ (s^{1+n})

$SM = 0.2281$ $(g\ s^{-1})$

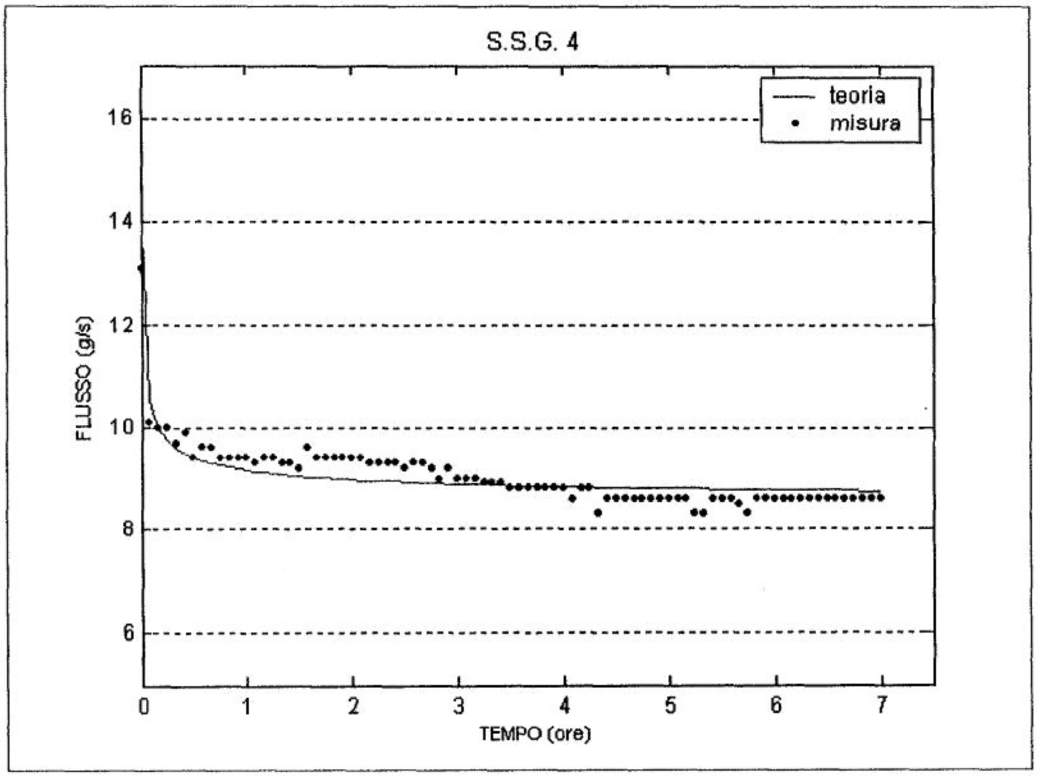

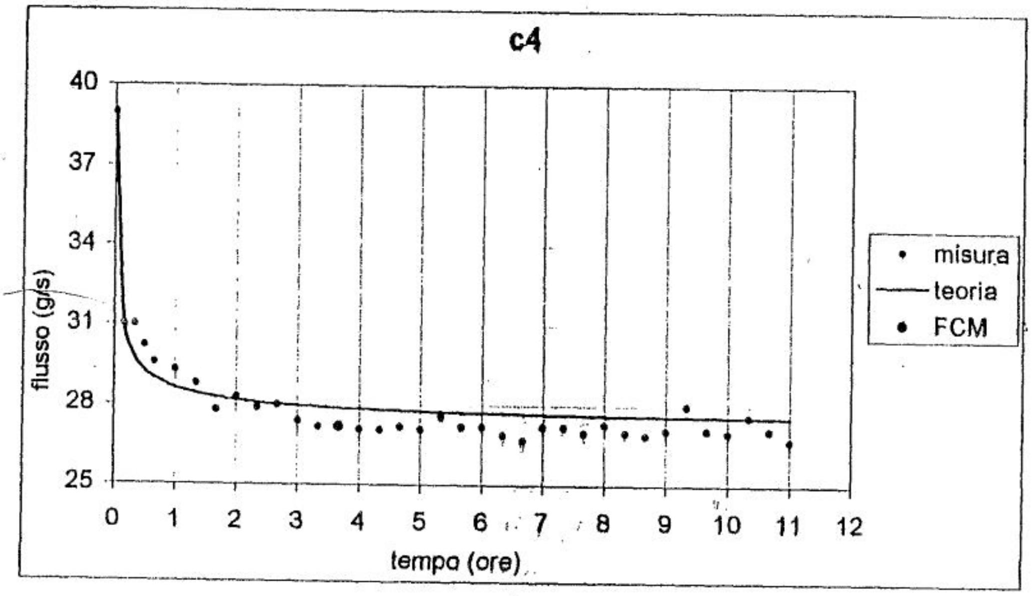
c4
40
37
34
31
28
25
flusso (g/s)
0
1
2
3
4
5
6
7
8
9
10
11
12
tempo (ore)
misura
teoria
FCM

Fig. 4.7

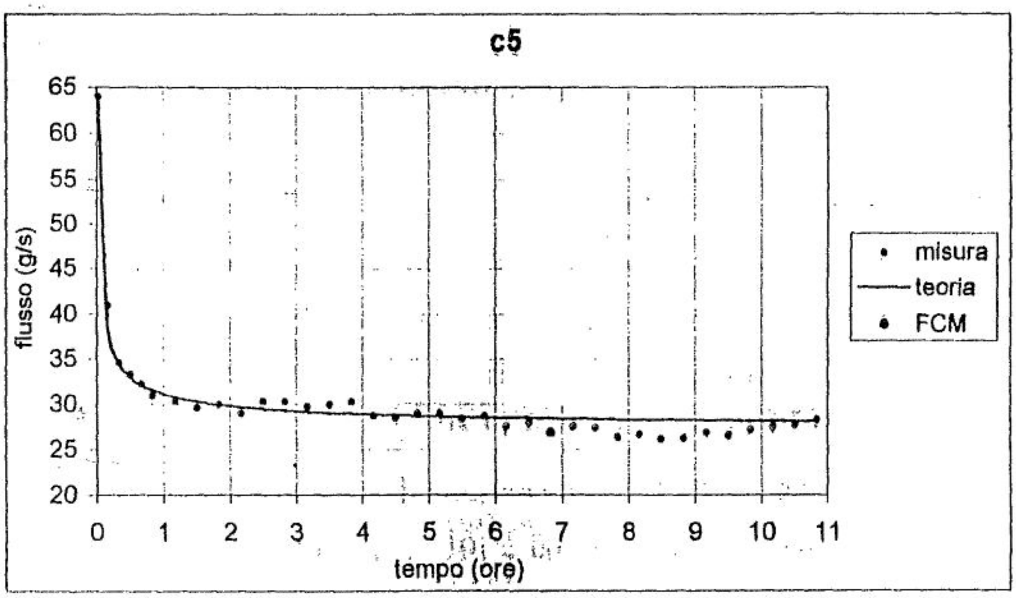
c5
65
60
55
50
45
40
35
30
25
20
flusso (g/s)
0
1
2
3
4
5
6
7
8
9
10
11
tempo (ore)
misura
teoria
FCM

Fig. 4.8